

# Field Demonstration of a 24-kV Warm Dielectric Superconducting Cable at Detroit Edison

*FY2003 Annual Progress Report*

**1002040**





# **Field Demonstration of a 24-kV Warm Dielectric Superconducting Cable at Detroit Edison**

*FY2003 Annual Progress Report*

1002040

Technical Update, March 2004

EPRI Project Manager

S. Eckroad

Pirelli Cables and Systems USA, LLC

The Detroit Edison Company

U.S. Department of Energy

American Superconductor Corporation

Lotepro

## **DISCLAIMER OF WARRANTIES AND LIMITATION OF LIABILITIES**

THIS DOCUMENT WAS PREPARED BY THE ORGANIZATION(S) NAMED BELOW AS AN ACCOUNT OF WORK SPONSORED OR COSPONSORED BY THE ELECTRIC POWER RESEARCH INSTITUTE, INC. (EPRI). NEITHER EPRI, ANY MEMBER OF EPRI, ANY COSPONSOR, THE ORGANIZATION(S) BELOW, NOR ANY PERSON ACTING ON BEHALF OF ANY OF THEM:

(A) MAKES ANY WARRANTY OR REPRESENTATION WHATSOEVER, EXPRESS OR IMPLIED, (I) WITH RESPECT TO THE USE OF ANY INFORMATION, APPARATUS, METHOD, PROCESS, OR SIMILAR ITEM DISCLOSED IN THIS DOCUMENT, INCLUDING MERCHANTABILITY AND FITNESS FOR A PARTICULAR PURPOSE, OR (II) THAT SUCH USE DOES NOT INFRINGE ON OR INTERFERE WITH PRIVATELY OWNED RIGHTS, INCLUDING ANY PARTY'S INTELLECTUAL PROPERTY, OR (III) THAT THIS DOCUMENT IS SUITABLE TO ANY PARTICULAR USER'S CIRCUMSTANCE; OR

(B) ASSUMES RESPONSIBILITY FOR ANY DAMAGES OR OTHER LIABILITY WHATSOEVER (INCLUDING ANY CONSEQUENTIAL DAMAGES, EVEN IF EPRI OR ANY EPRI REPRESENTATIVE HAS BEEN ADVISED OF THE POSSIBILITY OF SUCH DAMAGES) RESULTING FROM YOUR SELECTION OR USE OF THIS DOCUMENT OR ANY INFORMATION, APPARATUS, METHOD, PROCESS, OR SIMILAR ITEM DISCLOSED IN THIS DOCUMENT.

ORGANIZATION(S) THAT PREPARED THIS DOCUMENT

**Pirelli Power Cables and Systems, LLC**

**The Detroit Edison Company**

**U.S. Department of Energy**

**American Superconductor Corporation**

**Lotepro**

**This is an EPRI Technical Update report. A Technical Update report is intended as an informal report of continuing research, a meeting, or a topical study. It is not a final EPRI technical report.**

## **ORDERING INFORMATION**

Requests for copies of this report should be directed to EPRI Orders and Conferences, 1355 Willow Way, Suite 278, Concord, CA 94520. Toll-free number: 800.313.3774, press 2, or internally x5379; voice: 925.609.9169; fax: 925.609.1310.

Electric Power Research Institute and EPRI are registered service marks of the Electric Power Research Institute, Inc. EPRI. ELECTRIFY THE WORLD is a service mark of the Electric Power Research Institute, Inc.

Copyright © 2004 Electric Power Research Institute, Inc. All rights reserved.

## CITATIONS

This document was prepared by

Pirelli Power Cables and Systems USA, LLC  
710 Industrial Drive  
Lexington, SC 29072

Principal Investigator  
N. Kelly

This document describes research sponsored by EPRI, Pirelli Cables and Systems USA, LLC, The Detroit Edison Company, U.S. Department of Energy, American Superconductor Corporation, and Lotepro.

The publication is a corporate document that should be cited in the literature in the following manner:

*Field Demonstration of a 24-kV Warm Dielectric Cable at Detroit Edison: FY2021 Annual Progress Report*, EPRI, Palo Alto, CA, Pirelli Cables and Systems USA, LLC, Lexington, SC, The Detroit Edison Company, Detroit, MI, U.S. Department of Energy, Golden, CO, American Superconductor Corporation, Westborough, MA, and Lotepro: 2004. 1002040.



# **1 Introduction**

A project sponsored by EPRI, Pirelli Power Cables and Systems, the Department of Energy, Detroit Edison, and American Superconductor Corporation was initiated in 1998 to install and operate a 24 kV HTS power cable in a Detroit Edison substation to serve customer load. The previous years of activity have focused on design, testing, manufacturing, and installation of the cable system as described in the FY2000 and FY2001 status reports. FY2002 status report focussed on leak detection.

The cornerstone of this demonstration lies in the field application of HTS cable technology. The scope of this project will result in the world's first underground installation of a HTS cable system using an existing duct network. Furthermore, the project involves installing the necessary accessories on the project site within the constraints of a crowded distribution station.

Customer acceptance of HTS cable technology requires a substantial field demonstration illustrating both the system's technical capabilities and its suitability for installation and operation within the utility environment. This demonstration project has been designed to resolve many of the outstanding questions regarding the use of HTS power cables in utility networks.

This report summarizes the progress of this demonstration program between the dates of 2 December 2002 and 1 December 2003.

## **1.1 Acknowledgement**

The authors would like to acknowledge the accomplishment of this work through its partnership with the Department of Energy's Office of Power Technologies supported under cooperative agreement number DE-FC36-98GO10283. This support does not constitute an endorsement of the views expressed in this paper.

## **1.2 Project Description**

The demonstration cable circuit runs approximately 120 m between the 24 kV bus distribution bus and a 120 kV-24 kV transformer. This location for the demonstration site was selected because it combined performance specifications suitable for the application of an HTS cable circuit and several practical advantages. Though the route is not as long as is anticipated for commercial applications and is completely contained within Detroit Edison's property, it offered many challenges similar to those that will be faced in other field installations. Figure 1 shows the station layout and the installation route.

The 24 kV cables were designed and built using the Warm Dielectric (WD) design concept, which places the dielectric material outside the cryostat, so that it operates at ambient temperature. This enabled the use of a conventional dielectric, EPR, for the cable insulation. The system also proposed to demonstrate accessories, including terminations, an installation joint, and a repair joint. Figure 2 shows a cross section of the cable construction with its primary features visible.

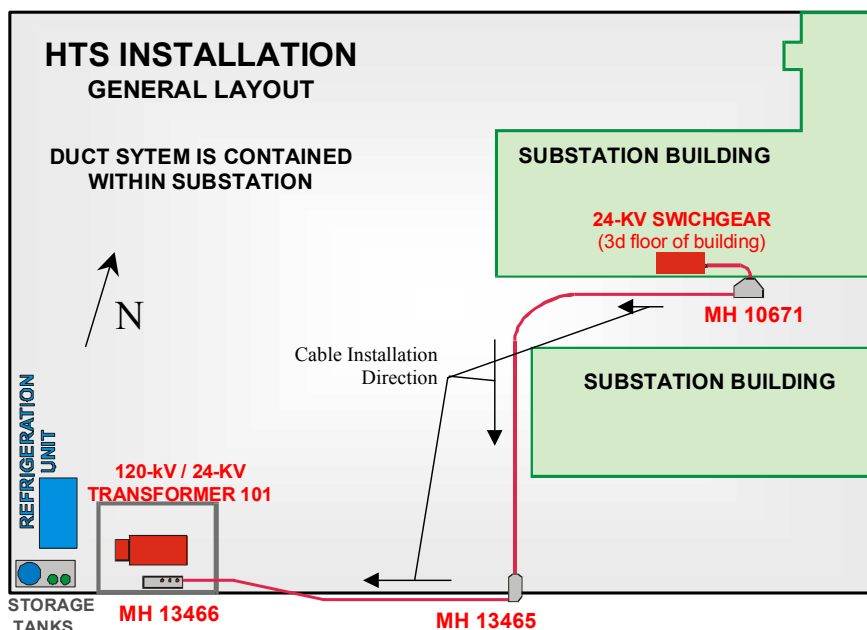


**Figure 1. Cable Site Layout**

Installing and operating an HTS cable system in an existing distribution substation represents the primary objectives for this program. The rigorous requirements imposed by field applications remain a critical element for proving the practicality of HTS cables. The Frisbie project site provided many challenges to the installation design, including small manholes, tight cable bend radii, and five bends along the route.

The system also includes vacuum and cryogenic support equipment that is new to the utility operator. Fully engineered and instrumented systems are used to minimize the attention required during normal operation. As this project remains a demonstration, the hardware employed may not totally represent that which will be used for future applications.

The first phase was the design and manufacture of the complete cable system (cables, accessories, refrigerator, and monitoring equipment), as well as the preparation of the substation site for installation. Most of the design and conductor fabrication activity was described in the 1999-2000 project update.

The second phase of the project emphasized the goal of demonstrating HTS cable systems in the utility environment. The cable and accessories designed and manufactured in the earlier phase



**Figure 2. Cable with Features Displayed**

were installed at Frisbie substation. The complete cable system was proposed to undergo commissioning tests for a period of time to verify the installation and establish a baseline for system behavior. The cable and accessory fabrication work and the installation of the system were described in the 2000-2001 volume.

Once fully commissioned, the plan established by the partners called for a basic operating period of two years. Two years was recognized as the minimum time needed to begin to appreciate the long-term behavior and reliability of the system.

In preparation of commissioning the system, vacuum leak testing was conducted; and leaks were discovered. The 2001-2002 volume describes the vacuum and leak detection phase of the project that encompassed all of 2002.

This report primarily covers the cryostat evaluation on Phases X and Z and the AC Loss Testing on Phase Y.

### **1.3 Project Partners and Activities**

An HTS cable system requires a fully engineered integration of three core technologies: HTS wire, power cable manufacturing, and cryogenic systems. The project team was formulated to provide expertise in all of the various aspects and components of HTS systems and their application to the electric power network.

- Pirelli Cables and Systems, the world's largest power cable manufacturer, was the project leader, as well as specified all subcontracted material and designed and manufactured the cable and accessories;
- American Superconductor Corporation provided the highest quality and performance BSCCO-2223 wire available;
- Detroit Edison provided the demonstration site as well as their perspective and expertise as an electric utility with significant Transmission and Distribution cable systems. Detroit Edison field personnel also worked on the installation and commissioning of the systems;
- EPRI contributed their overall industry perspective and experience introducing new technologies to the utility industry;
- Los Alamos National Laboratory provided experimental evaluation of AC losses in conductor assemblies; and
- Lotepro Corporation engineered and manufactured the cryogenic refrigeration system.

The work was supported under Phase Two of the Department of Energy Office of Energy Technology's Superconducting Partnership Initiative (SPI).

## **2 Vacuum Leak Detection and Location**

### **2.1 Initial Detection**

After the installation of the cable, refrigeration system and accessories was complete in late December 2001, tests were conducted to prove the integrity of the vacuum system in

preparation for the power-up of the system. The cables' cryostats were purged with CO<sub>2</sub> and then were connected to pumping groups. After about one month of pumping, the residual pressure was not satisfactory in any of the phases, indicating possible leaks.

Therefore, pressure variation response tests were conducted on each conductor phase. Using different pumping groups, the cryostats and conductor space inside of the inner corrugated tubes were evacuated. After evacuating the conductor space (thereby minimizing leaks between the conductor space and cryostat), an improvement in vacuum level of phases X and Z was recorded. All the conductor spaces were pressurized with gaseous nitrogen (GN) @ 1.6, 2.6 and 3.6 bar. An immediate vacuum pressure response was recorded on phases X and Z. Before increasing pressure in the conductor space from one level to the next, the pressure in the cryostat was allowed to reach a plateau. Pressure was monitored from each end of the cryostats. See Figure 3. Note that Vacuum gauge X out was not working properly.

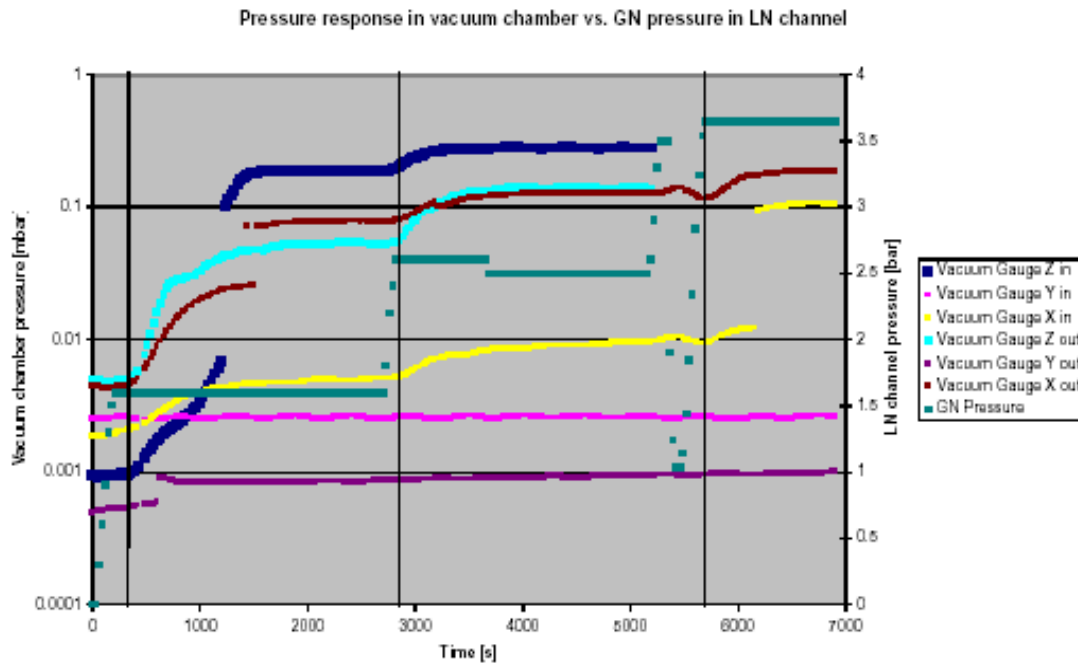


**Figure 3. Pressure response in vacuum chamber**

From this test the team concluded that:

1. Phase X and Z vacuum gauges' response could give an indication on leak position, but their responses being almost equal in time but at different level, could indicate:
  - Leaks of different size on both terminations;
  - Leak inward on phase Z and outward on phase X.
2. Phase Y didn't show any response to pressure variation.

In order to further identify the size and leak locations in Phases X and Z and to confirm there were no leaks in Phase Y, a helium (He) diffusion time test was conducted. The cryostat of each phase was evacuated, and the He background level was measured with a mass spectrometer

(Pfeiffer QvalyTest) connected at one end (sec. I). Then the He leak rate and the He diffusion time was measured, pressurizing the inner corrugated tube @ 1 bar. The test was repeated, moving the mass spectrometer to the other end of the cryostat (sec. 3) and then for each phase.

These tests showed that both Phase X and Phase Z had probable large leaks close to the indoor termination end of the cable, and that Phase Y had a probable small leak close to the indoor termination end of the cable.

After evaluating the data from these tests, it was determined that at least partial disassembly of Phases X and Z was required to further investigate the criticality of the leaks and to determine if the leaks were repairable *in situ*. This further investigation necessitated both design of the tests and components so as to be able to reassemble the cable phases after the tests were conducted and leak repaired, if possible.

## **2.2 Phase X - Investigation**

In particular, quality tests on the inner corrugated tube from short lengths of cable, which were connected to the pulling head during the initial cable installation and subsequently cut from the cable and returned to Italy, were conducted in February 2002. These short lengths had experienced the worst installation loading.

The He leak test was performed on some samples of inner corrugated tube. These tubes were taken from the extra length of the installed cable near the cable head. The aim of the test was to verify statistically if any damage occurred to the longitudinal weld as a consequence of cable installation. All the components were tested with He sniffer and the He spray method, both methods being based on a mass spectrometer analysis. Neither the spray nor the sniffer methods showed any detectable leak in the longitudinal weld of the inner corrugated tube. Therefore it was concluded that leaks, if existing, were lower than  $1 \cdot 10^{-8}$  mbar/s.

Further, thermal inertia tests on the cryostat with low vacuum pressure were conducted in February/March of 2002. This test was carried out on a 3-meter long cable sample. Three holes at 120° apart around the longitudinal axis of the cable were drilled in the triple insulation of the cable close to the two ends and in the middle of the sample. Nine thermocouples were placed in these holes to monitor EPR temperature during the cooling down. The liquid nitrogen (LN) channel was then filled with LN, with varying pressures in the cryostat. The goal of the test was to evaluate the cool-down time of the triple extrusion inner surface under conditions in which a good residual pressure cannot be assured (due to cryostat leaks). That is, it was desired to determine whether cryo-pumping could ensure a good residual pressure level. We found that for a residual pressure higher than  $10^{-3}$  mbar, heat conduction due to residual gas is high enough to cool EPR temperature down to 250 K in approximately 4 hours. This result indicated that it would be almost impossible to safely perform electrical tests on the installed cables.

All the components that would be needed to reassemble the cables were designed. Furthermore, five test chambers were designed, purchased, tested with few modifications required. The chambers were designed for use in the leak detection activity in Detroit. In particular, the investigating technique consisted of removing from the termination's outer jacket one piece at a

time, providing separation between sections with removable seals. This technique required cuts, temporary components and welds for the reconstruction. Care had to be taken during the cut phase in order to reduce vibrations and to leave a safe and wide enough area to work with the temporary chambers needed for the test. The cutting device, method and the test chambers were tested in Milan for efficiency, providing an opportunity for a design review of the tools. In fact, a few modifications were necessary. The main modifications were done to obtain an easier fit of cutting tools on the terminations and good sealing performance. Two main challenges were overcome: narrow spaces to fit temporary test chambers, and seals on orthogonal faces. The test showed a sufficient fit for the chambers and good behavior of the seals.

These components were sent to the Frisbie site and investigation was begun and completed on Phase X. Figure 4 is used as a reference diagram for describing this investigation.

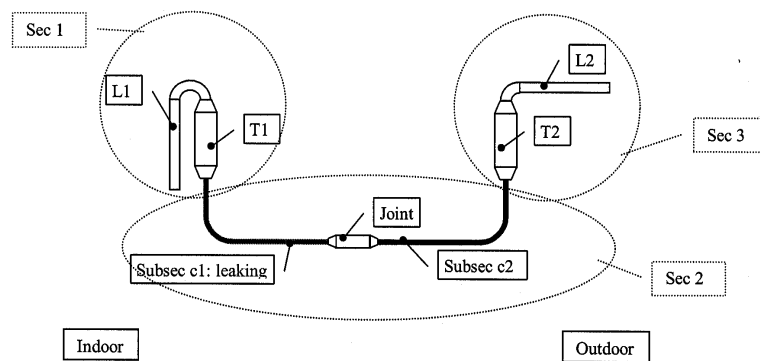


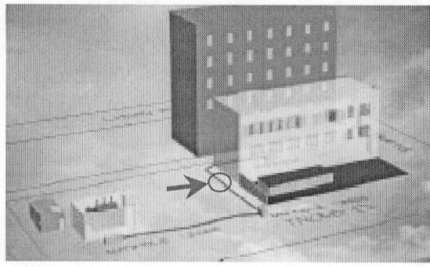
**Figure 4. Test sections and subsections**

A summary of the leak detection tests described above for Phase X is shown in Table 1. (Refer to Figure 4 for section locations).

**Table 1**

Test Section	Subsec.	He Leak Results
1	L1	Passed
	T1	Passed
2	C1	<i>Failed</i>
	Joint	Passed
	C2	Passed
3	L2	Passed
	T2	Passed

In conclusion, the tests indicate that the leak(s) should be located approximately 16-22 meters from the splice, or 42-48 meters from the indoor termination, as illustrated on site diagrams (Figures 5 & 6 below).



Estimated leak position

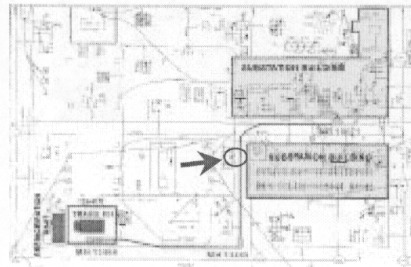


**Figure 5. Leak position – perspective.      Figure 6. Leak position - plan**

In addition to the qualitative results on leak existence, tests were conducted to establish:

- Vacuum response in the cryostat to pressurization of LN channel with GN; and
- He flight time on section and subsection of cable.

This data was used to estimate the position of the leak(s).

Further, these tests showed:

- The estimated conductance from the leak position to L1 is below  $2 \text{ m}^3/\text{h}$ , reducing the pump efficiency from the leak from  $40 \text{ m}^3/\text{h}$  down to  $2 \text{ m}^3/\text{h}$ ; and
- Minimum reachable pressure in the joint chamber with LN channel pressurized @ 4.6 bar with GN is 1.5 mbar with a leak rate of 0.196 standard cubic centimeters per second (sccs).

It was determined at this point that Phases X and Z, which had the large leaks, should be removed and shipped to Milan for dissection and analysis in the lab to confirm location and determine the root cause of the leak mechanism. While the tests reported above indicated that the EPR insulation would have suitable dielectric performance even at low temperatures, vacuum and safety issues precluded cooling down and energizing these two phases, leaks notwithstanding. Phases X and Z were therefore removed and shipped to Milan for dissection and analysis.

Thus the plan was to replace Phases X and Z with conventional cables, install return LN piping and operate the system with one HTS phase (Phase Y) and two conventional phases. However, before implementing this plan, it was decided to conduct some further tests on Phase Y to ensure the leak was stable.

## 2.4 Phase Y Investigation

Test activity at the Frisbie substation on Phase Y during this period consisted of thermal and mechanical cycles: cool down; pressurization; leak test; warm up; leak test.

An ordered list of leak tests was performed as follows:

1. He leak test @ Room Temperature (Warm He Test)
2. Cable Cool down
3. He leak test @ almost LN Temperature (Cold He Test)

4. Cable warm up
5. Warm He Test
6. Cable Cool down
7. Pressurization cycles with LN: ambient pressure – 159 psi – ambient pressure – 159 psi – ambient pressure
8. Cold He Test
9. Cable warm up
10. Warm He Test
11. Cable Cool down
12. Pressurization cycles with LN: ambient pressure – 159 psi – ambient pressure – 159 psi – ambient pressure
13. Cold He Test
14. #2 Warm He Test

After each He test, the cryostat and inner corrugated tube were purged for 30 minutes with GN to remove residual He.

The overall result was a small degradation of the leak after three thermal cycles and 4 pressurization cycles; the final He leak rate was about  $4.5 \times 10^{-4}$  sccs, 30% higher than the previous rate. The absolute value of the degradation was about  $1.4 \times 10^{-4}$  sccs.

Before the first cool down a leak test was performed to verify the initial state of the HTS cable. The value obtained through this test was consistent with the leak levels measured during previous testing activities.

There was no evident change in the test results after the first and the second cycle, but after the third and last cycle tests the cable demonstrated a leak rate increase up to about  $4.5 \times 10^{-4}$  sccs (about 30% more than initial value  $3.4 \times 10^{-4}$  sccs).

The remaining middle HTS phase (Phase Y) was cold tested. It withstood two thermal and mechanical cycles without showing any increase in He leak rate, but during the third and last cycle an increase in leak rate occurred.

It was concluded that *theoretically* with this leak rate, it might still be possible to operate the cable. However, because there was some degradation of the leak rate after cycling and because the vacuum leak evolution could not be accurately predicted, some minor modifications to the vacuum connection and further tests would have to be performed before making any final decision about operating Phase Y.

The goal of further testing on Phase Y during this period was to have an estimation of leak evolution and an estimation of the increased safety margin in vacuum level thanks to the added pump capacity of pumping groups previously dedicated to Phase X and Z. In fact, because of Phase X and Z removal more pump capacity was available; moreover the turbos were placed closer to the ceramic insulator, providing greater safety margin. Furthermore a vacuum gauge was located very close to the ceramic insulator, reducing uncertainty on vacuum level between the coaxial ceramic insulators.

Phase Y was submitted to a longer-term pressurization cycle, 120 psig for 24 hours at cryogenic temperatures. During this pressurization, a stable vacuum level was obtained with no increase in leak rates. Phase Y was then warmed-up and submitted to a He leak check. The data from the He leak check showed the leak rate had changed, showing continued instability in the leak.

## **2.5 Results and Conclusions From These Tests**

- A.** The results of the longer-term tests to Phase Y showed that the warm leak rate is not stable – confirming the leak had the potential for increase. The nature of the leak was that it was unstable. Therefore it was unpredictable how the leak would evolve under operation.
- B.** The leak required vacuum systems to be running continuously. The vacuum systems were designed as a secondary system providing back up service. They were not designed using N-1 failure criteria, as would now be required. Thus, these secondary systems would be required to run continuously as a critical component.
- C.** If there would be a vacuum failure, even if the control system operated properly, it would be necessary to de-energize a transmission feeder to isolate the test cable from system voltage. While this operation can be automated, the process could be intrusive on network operations.
- D.** Based on the above, it was Pirelli's recommendation, and confirmed by the team, that Phase Y would not be put into operation in the electrical grid.

## **3 2003 Activities: December 2, 2002 – December 1, 2003**

### **3.1 Dissection and Analysis of Phases X and Z Leaks**

After removing the two superconducting cables comprising Phase X and Phase Z of the three phase circuit, a number of sections were taken from the cryostat's inner tube for metallurgical analysis. The individual sections removed were identified as having leaks identified using mass spectrometry.

#### **3.1.1 Microscopic Methodologies**

Using He mass spectrometry, leaks in the inner cryostat tubes were located. Four sections of the cryostat around leak locations, each approximately 0.4 m in length, were removed and taken to the laboratory for microscopic analysis. The position of each of the four sampled sections, as they would have been located at Frisbie is noted in Figure 7.

The samples were examined as received using an optical stereomicroscope. Cracks located by this method were prepared and examined using both optical and scanning electron microscopes.

Metal morphology inside and outside the weld region and the characteristics of individual defects were analyzed to provide clues regarding the root cause of the cryostat failures.

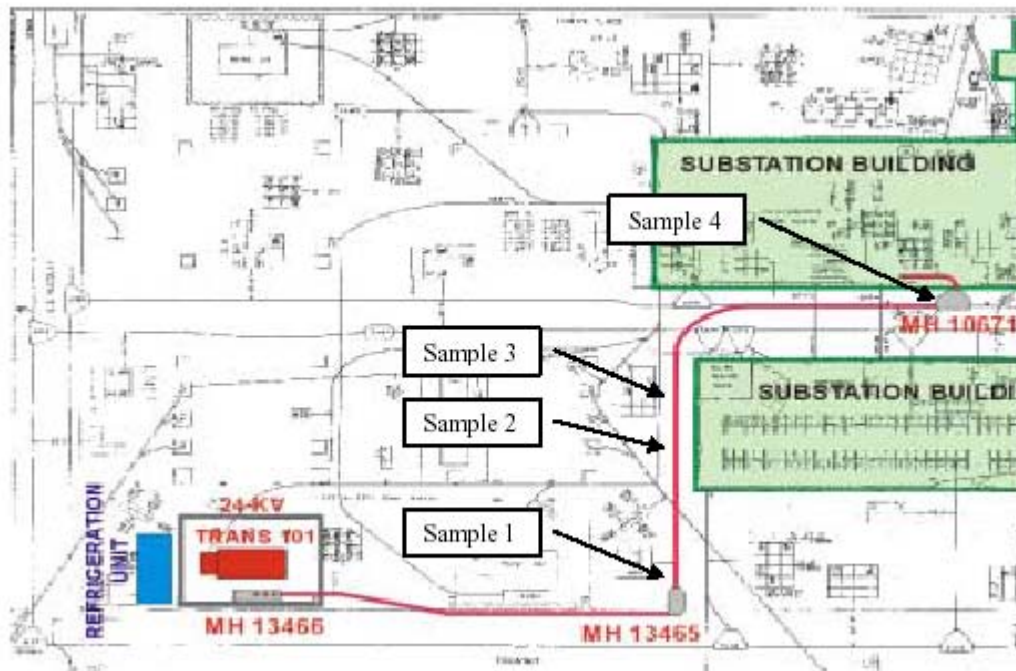


**Fig. 7. Samples location**

### Macroscopic Inspection

The samples were initially given a preliminary inspection, as they were received, using an optical stereomicroscope.

### Optical Microscopic Inspection

Most of the optical observations were carried out after micrographic preparation (cutting and polishing) and chemical etching, to better analyze the crystalline features of the steel tube. In the following, the different samples will be identified according to the number of the tube from which they were taken.

### SEM Inspection

The outer and inner surfaces of the tube samples were observed at different magnifications using a scanning electron microscope (SEM). Details of the cracks and other small defects were also observed at high magnification after optical preparation.

## **3.1.2 Results**

### Macroscopic Location of Cracks

By this method, a few micro-cracks were identified on the outer surface of the tube. These cracks were examined in deeper detail by optical and SEM microscopy. All the observed micro-cracks were found to be oriented parallel to the axis of the tube and to be localized inside a corrugation groove along the welding line.

### Morphology of the Cracks

The pictures taken using the SEM best document the appearance of the defective spots. As can be seen in the example Figures 8 to 13, the largest cracks were all found to extend parallel to the axis of the tube, and to be typically visible on the outside surface.

In all the above documented cases, the cracks seem to have initiated from the outer surface, where there appears to be a small and smooth V-shaped groove. Such a feature, which is better evident from the micrographic optical observation, was searched for in other parts of the welding along the tube, inside other corrugation grooves adjacent to the crack location, and found to be absent.

A weld line, due to the complex flow of the material during cooling, is not in itself a totally uncommon feature in some metal systems and under some conditions, in this particular case this is only found occasionally, and seems to be a local indicator of a defective spot.

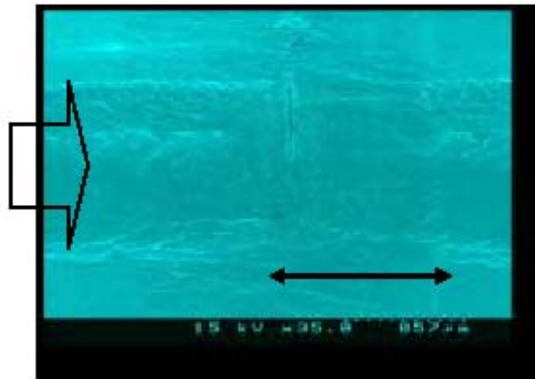


**Fig. 8. Tube sample 4, crack along the welding.**

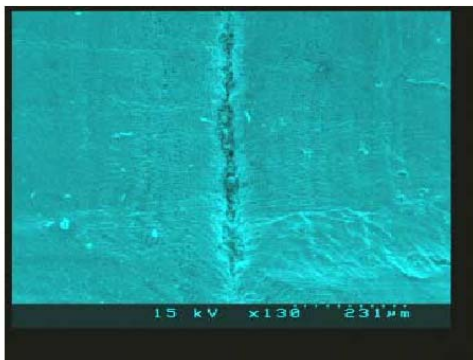


**Fig. 9. Tube 4, detail of the crack.**

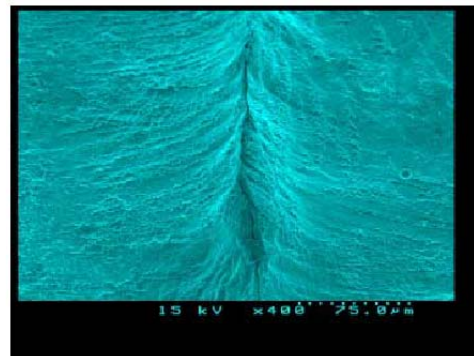


**Fig. 10. Crack in tube 1**



**Fig. 11. Crack in tube 2**

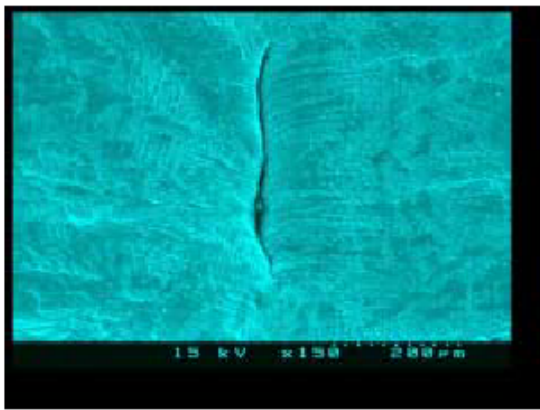


**Fig. 12. Crack 3-1 in tube 3, outer surface**

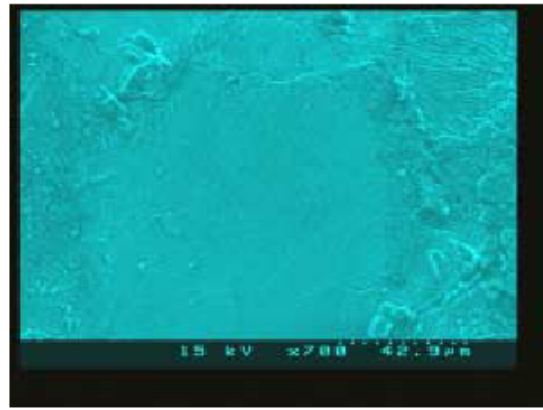


**Fig. 13. Crack 3-1 inner surface, detail**

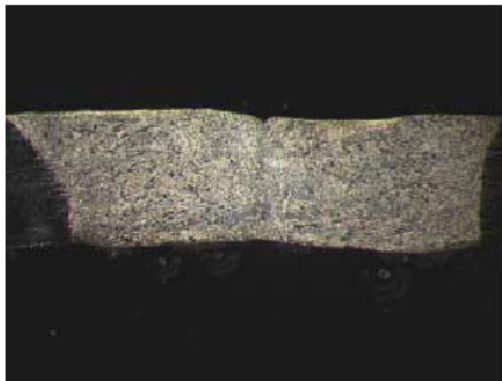


**Fig. 14. Tube 3 - crack location**

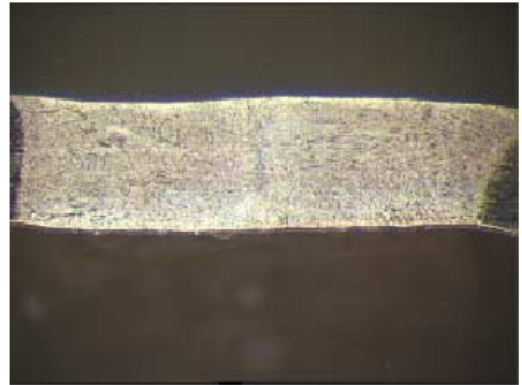


**Fig. 15. Tube 3 - a few mm from crack**

### Metallographic and SEM observation

A number of samples taken to include the largest surface cracks, as well as a sample taken from a “good” part, were given a standard metallographic preparation to expose a normal cross-section including the crack. The polished and chemically etched samples were then observed at different magnifications. Figures 16-18 show the only sample where the crack is actually visible in its complete extension.

As can be observed, the fracture line, which is located quite in the center of the weld (the anvil-shaped, lighter region in Figure 16), is rather “broken”, and seems to suggest that the fracture might have occurred in two steps. The crystalline structure that is well visible at higher magnification (shown in Figure 16) does not show particular anomalies, and is quite similar to the one found in other samples taken from a non-defective welding region.

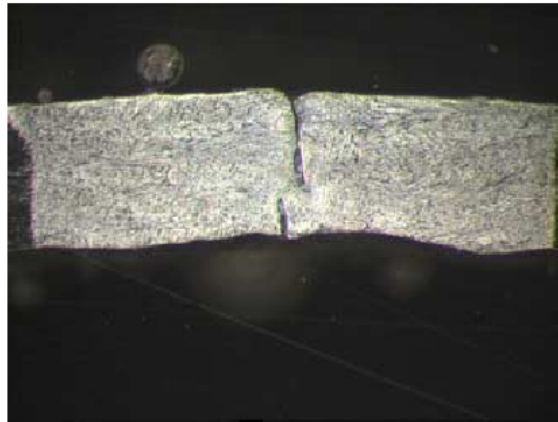


**Fig. 16. Crack in tube 1**

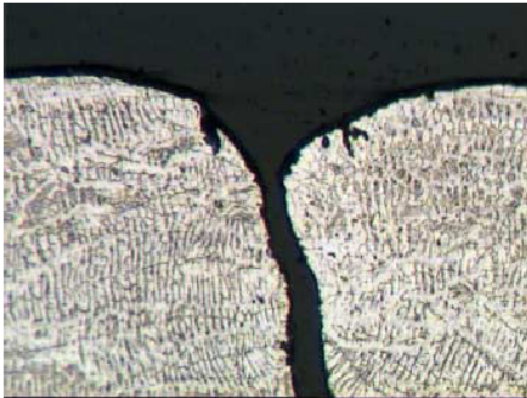


**Fig. 17. Tube 1, detail of crack on outer surface**

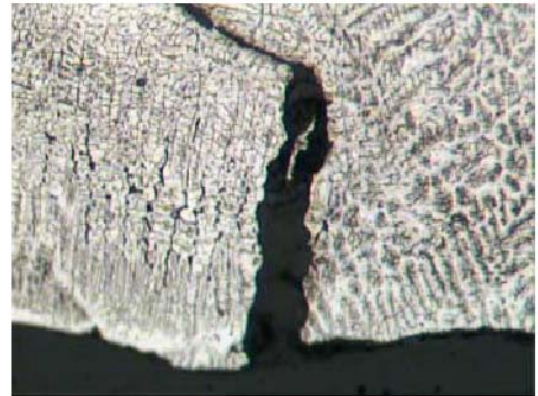


**Fig. 18. Tube 1, detail of crack on inner surface**

The metallographic structure in the welding zone is a two-phase dendritic, while the tube at the weld boundary has a single-phase structure. The two-phase structure is due to ferrite formation along with the original austenite, confirmed by observing a slight magnetic attraction at the weld while the rest of the tube is definitely non-magnetic.

All the observed cracks strictly follow the interphase boundaries. This is supported by SEM observations of cracks opening at the outer surface (see Figures 19 and 20) showing interphase boundaries (dendrite nodules in Figure 21). This indicates that these defects were formed during the solidification process.

The actual cause for these defects is not completely clear. The distribution of these defects shows, on the contrary, a very localized pattern (defects were never found in adjacent sections). This is evidence in favor of an origin due to material characteristics rather than welding process anomalies.



**Fig. 19. Tube 1 detail of crack on inner surface**



**Fig. 20. Tube 4 outer surface**

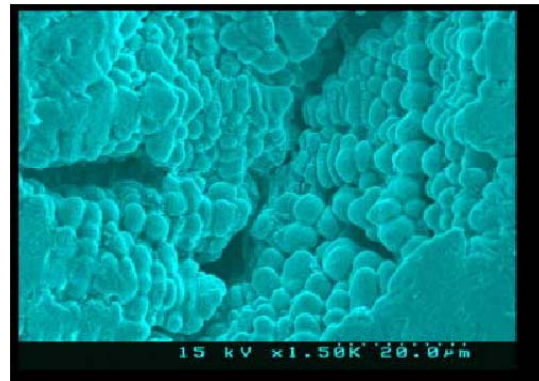


**Fig. 21. Tube 4, detail of crack shown in Fig.20**

In particular, the hypothesis of excessive gaseous content is worth evaluating. In fact it could explain some peculiar aspects like inner bulk location of incipient defects, their interphase boundary contour and their association to “macroscopic” shrinkage. Another point worth considering is the systematic location of the defects in correspondence to the corrugation grooves. Corrugation is the result of cold working after welding, which by no means could “attract” the defects formed by solidification shrinkage and cause them to localize.

In fact a perhaps more likely, alternative picture to that of a “pure” solidification shrinkage effect, comes by considering a hydrogen embrittlement mechanism. Under this theory, defects would have developed under the action of the corrugation stresses at random locations rich in hydrogen (it is known for instance that martensitic stainless steels show marked brittleness at room temperature with 3-5 ppm H<sub>2</sub>). In this hypothesis the damage is interpreted as a mechanical-stress-driven brittle propagation of cracks along hydrogen polluted interphase boundaries generated during welding. These fractures must be supposed to have been originally incomplete, having not been detected during manufacturing. They would eventually develop to the full thickness of the tube when further stress was applied.

Partial support to the above came from the additional observations that were carried out on a sample taken from a non-defective region of tube 1, from outside the welding and outside the corrugation groove. Careful metallographic observation in this sample showed also the presence of tiny defects like the ones shown in the Figure 22-25.

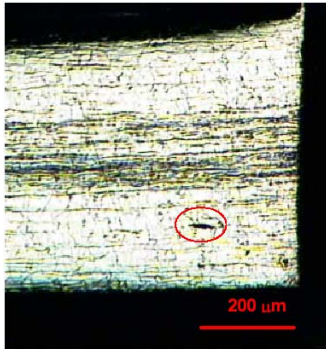


Fig. 22. Tube 1, outside the welding

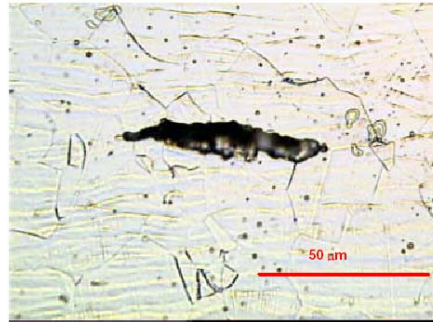


Fig. 23. Tube 1, detail of the defect in Fig. 22

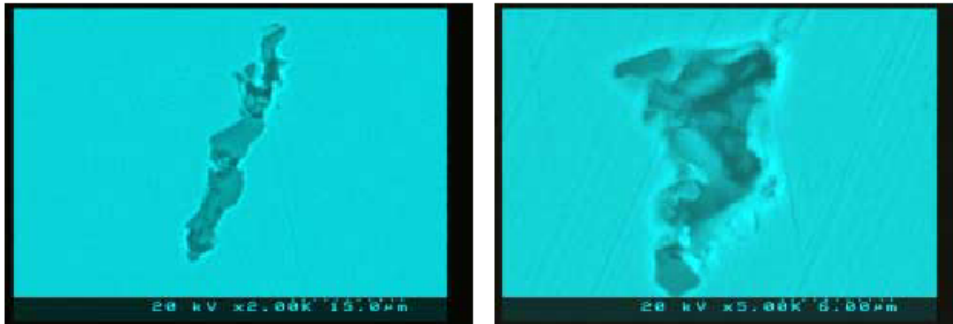


Fig. 24-25. SEM pictures of defects in tube 1, outside the welding and outside the corrugation groove

### 3.1.3 Summary and Conclusions for Leak Analysis

Microscopic analysis of the leak locations revealed that nearly all of the leaks occur near the middle of the weld seam in the cryostat corrugations, at micro cracks that were oriented parallel to the weld direction. The weld seam in correspondence to the defects has a slight depression in the middle along the weld direction probably caused by the complex flow of metal during the welding process.

In one case it was possible to prepare a metallographic sample that included a crack in its full extension. The fracture path followed a broken line, strongly indicative that the crack was formed in two steps. This suggests that the fracture may be due to the combination of a mechanical stress and a defective, weaker point in the welding region.

Some data suggests that the material might have been originally affected by anomalous hydrogen content, which would have in turn given rise to hydrogen-rich, brittle interphase boundaries during welding solidification. Incomplete fractures would then have been formed due to the mechanical stress of the corrugating process, and would eventually develop to the full thickness of the tube when further stress was applied.

## 3.2 AC Loss Testing

In order to test the characteristics of the superconductor element of the cable it was decided to arrange for phase 2 to be energized at low voltage, unconnected to the grid. Phase 1 and 3 had been removed from the underground ducting and 6 copper cables installed. The cooling system was simplified in that saturated (boiling) liquid nitrogen was passed along phase 2 in one direction and then vented to atmosphere.

### 3.2.1 August 2003 Tests

The HTS cable system was to be available for 5 days for testing in the period August 4 – 8, 2003. Planned activities were as follows:

Day	Planned Activity
1	Cryo check out DC power supply connection Instrument connection
2	Cool down Dc check out Computer control check out
3	DC $I_c$ measurements Rewire for ac Ac supply check out Ac loss instrument connection
4	Ac Loss measurement
5	Ac Loss measurement

#### Cooling

The cable was cooled on Day #2 of the tests without any problems. The vacuum jacket had been pumped continuously for at least a week prior to this and was pumped during test period. The cable achieved a stable temperature with an inlet pressure of 2.8bar and temperature of 86K. The saturated two-phase liquid nitrogen flow, along with the high heat leak of the cryostat due to poor vacuum, conspires to produce a very complicated cryogenic system. Thermometry on the cable showed that the temperature decreased between the nitrogen inlet and outlet. At the 110-meter point the temperature was approximately 82K, 4K lower than the inlet. This was due to the pressure gradient along the cable. As the pressure reduced towards the exit (at the 'inside' end) the saturation temperature decreased, liquid nitrogen would then vaporize to keep the two-phase flow on the saturation line.

### DC Energization

In order to energize the cable with dc current, six 875A, 5V dc power supplies were shipped from Pirelli, Milan for connection in parallel. The dc current was to be passed along the cooled HTS cable and returned via the 6 copper cables connected in parallel. In this circuit the maximum system voltage available was 5V and maximum possible current 5250A dc. In initial tests it was discovered that the cabling provided to interconnect the DC power supplies and to connect to the cable terminations had too high resistance (given the 5V limit on the power supplies). A considerable effort was expended on Day #2 to shorten all these cables and double them up, to enable the power supplies to drive sufficient current through the system. The experimental set-up is shown in Figure 26.

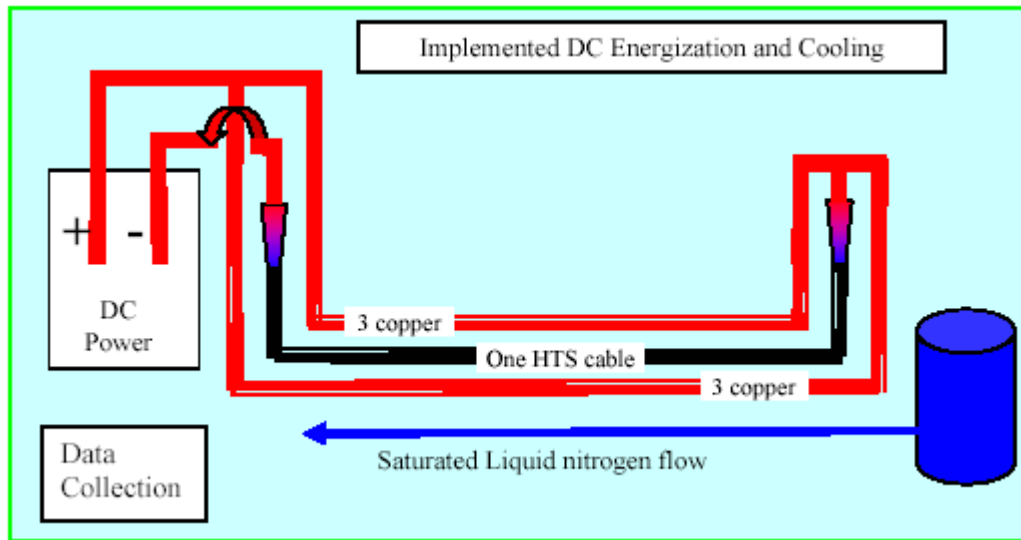


**Figure 26. DC Test Configuration**

### Instrumentation

Voltage taps were available along the cable at the zero-, 10-, 40-, 70- and 110-meter points in order to pick up the generated voltage. At each point there was a pair of wires to provide redundancy in case of failure. These taps were placed during cable construction and could not be changed or adjusted in any way during the tests. The eight voltages were to be recorded using a computer controlled, scanning nano-voltmeter, which also was to control the six dc power supplies. Four pairs of thermometers were also placed at intervals along the cable.

### **3.2.2 DC $I_c$ Tests**

Initially the dc power supplies did not function fully as the supplies were internally set for European input voltage levels. All six supplies had to be dismantled for their bus-bars, cases removed and internal connection re-made.

It was also discovered that the required computer control was not implemented. After some effort it was decided to abandon all attempts to control the systems via software and everything was re-wired for manual control and data acquisition. Progressive failures of thermometry also reduced the number of temperature data points available.

## DC Results

Figure 27 shows the DC voltage measured at various points along the cable, all measurements are referenced to the voltage taps at '0 meter'. Note that the data is taken at slightly different temperatures due to the temperature variation along the cable. Also it should be noted that all these data are the voltage difference between that point and the '0 meter' point of the cable. For example, the '110-meter' voltage *includes* the '70-meter' voltage values. The noise on these measurements is significant, mainly due to the electrical environment in the Frisbie substation. Given more time it would probably have been possible to collect better data. The 10-meter and 40-meter data seemed particularly noisy.

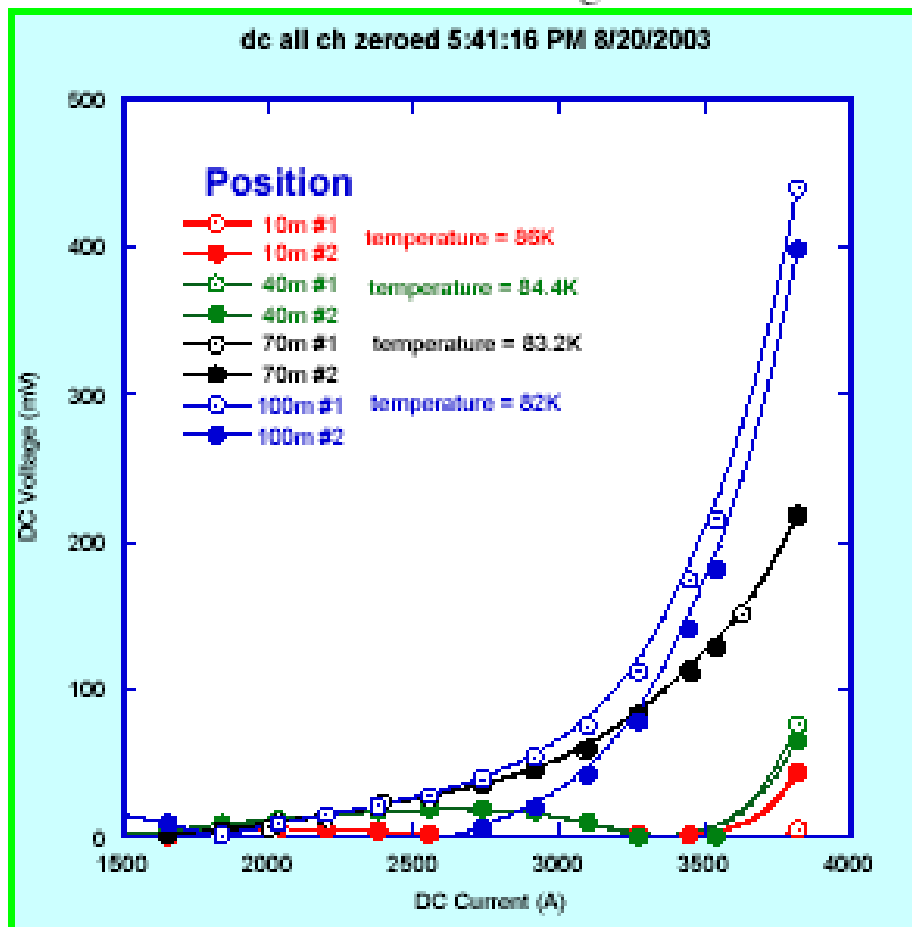


Figure 27. DC Test Results

On a 100 meter cable the critical current level of 1 microvolt per cm would yield 10 mV. Closer examination of the data presented above indicates that the critical current of the cable was approximately 2000 A at this temperature range. If we scale this to 77 K we might expect a critical current of 2800 A. There is some indication that a lower  $I_c$  region exists in the section between 40 meter and 70 meter (the 100 meter and 70 meter data show very similar behavior at currents below 2500 A, while the  $I_c$  up to 40 meter seems significantly smaller). However, the noise in the measurement makes this a tentative conclusion.

During these measurements no significant change in the cable temperature was noted.

### 3.2.3 AC Loss Tests

#### AC Energization

The cable was energized in 3-phase configuration using the two installed “copper” phases in place of the non-operational HTS phases. The three phase conductors were connected to the low voltage side of a delta-wye transformer located at the ‘outside’ end of the cable. This transformer had a turns ratio of 8:1. The ‘inside’ ends of the three phase conductors were shorted together using a copper bus bar. This common point was linked to the neutral of the transformer winding using a copper cable. This allowed the return of any imbalanced current. The HTS cable shield was grounded at the ‘outside’ terminal, this was the only ground point in the circuit. The configuration is shown in Figure 28.

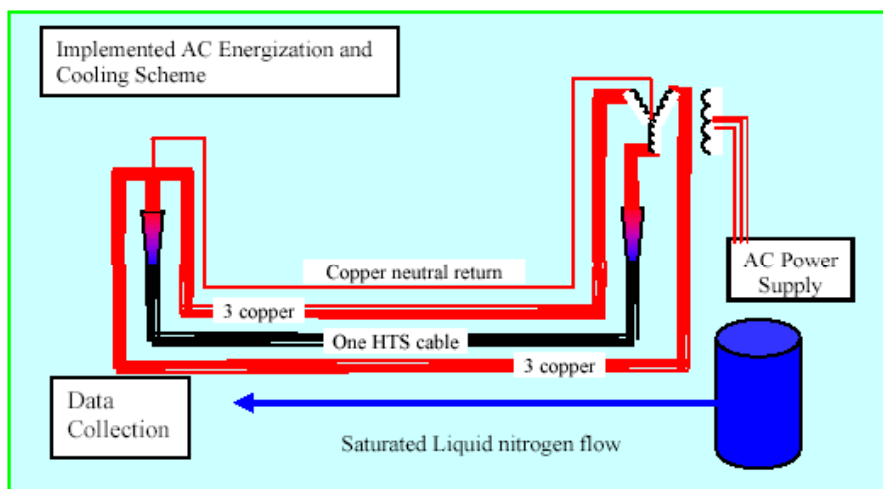


**Figure 28. AC Test Configuration**

The delta side of the transformer was connected to an inverter based power supply provided by American Superconductor Corporation, fed by the Detroit Edison 480V, 3 phase line supply. Although the ‘resistance’ of the circuit is low, about 60V ac was required to drive the required currents due to the inductance of the system. The outputs of this power supply were floating from ground.

#### Instrumentation

In order to measure the ac losses of an HTS cable it is necessary to make a phase sensitive voltage measurement. This is done using a lock-in amplifier (LIA). An LIA depends on a reference signal to provide frequency and phase information. This reference must be a very clean sine wave in order for the LIA to “lock”.

The team attempted to obtain a reference signal from a transformer placed on the HTS phase and alternatively from the resistive signal generated on the copper phases. The waveform from the AC power supply was highly distorted, with numerous high frequency components. Visually, the current sine wave had 3.5 kHz spikes superimposed (this was a breakthrough from the switching frequency of the supply) and was more akin to a square wave at 60Hz frequency. One possible reason for this distortion was the highly imbalanced 3-phase circuit this test represents. Two phases are copper low voltage conductors, with just a thin rubber insulating

covering. The impedance of these phases would be largely resistive. The HTS phase would have low resistance but significantly higher capacitance (it has a high voltage dielectric and a ground shield). Some idea of the imbalance of the system comes from the observation that, at an operating current of 600A per phase, an imbalance current in the neutral return of 80A was measured. The power supply was designed for a balanced three-phase load.

The team was unable to force the LIA to lock to 60Hz in the presence of so much 3.5 kHz on the reference signal, except at the highest amplitudes. In addition the voltage returned by the LIA only makes sense, as a “loss voltage” if the current wave form is a clean sine wave. After considerable effort the team abandoned all attempts to measure the losses electrically. It is believed this measurement could be done but only with a much ‘cleaner’ power supply.

As an alternate method to measure losses, LANL had developed a calorimetric technique. This utilized the difference in the electrical permittivity between liquid and vapor nitrogen to measure the vapor/liquid ratio in the coolant flow. In principle the energy losses could then be calculated from knowledge of the temperature and specific and latent heats of liquid nitrogen. This technique had worked well in the lab but failed in the field. The reasons for failure were twofold;

1. The extremely high background losses due to the poor thermal insulation on this cable (estimated to be about 2 orders of magnitude higher than the ac losses we were attempting to measure).
2. A liquid flow impedance near to the exit of the cable, this essentially vaporized much more liquid than the ac losses and swamped and measurement.

### AC Results

Neither of the intended ac loss measurement techniques yielded any data. During the attempts to make these methods work though, it was noticed that the cable temperature did change slightly when the ac current was applied, this was not seen during the dc tests. In Figure 29 we show the cable temperature rise at the 100m point along the cable (i.e. 100m from liquid nitrogen inlet).

The reason for the increase in temperature is not straightforward. The liquid nitrogen is boiling at all points along the cable; consequently an increase in temperature indicates an increase in pressure at that point. A higher pressure in the cable indicates higher viscosity in the two phase liquid flow downstream, caused presumably by a greater percentage of vapor in the flow compared to liquid – due to the higher heat input from the ac losses. In principal some estimate of the ac losses could be made from this data, but this was not thought to be worthwhile as it would be very approximate. Moreover, given the distorted waveform of the current the results would not be meaningful (there are many frequency components present, most particularly the 3.5kHz). However, some *minimum* value for the losses can be given. If we assume all the ac loss energy is used to raise the temperature of the two-phase liquid nitrogen flow, and not to vaporize more liquid, we find losses of approximately 35W for the whole cable length at a transport current of 2500A.

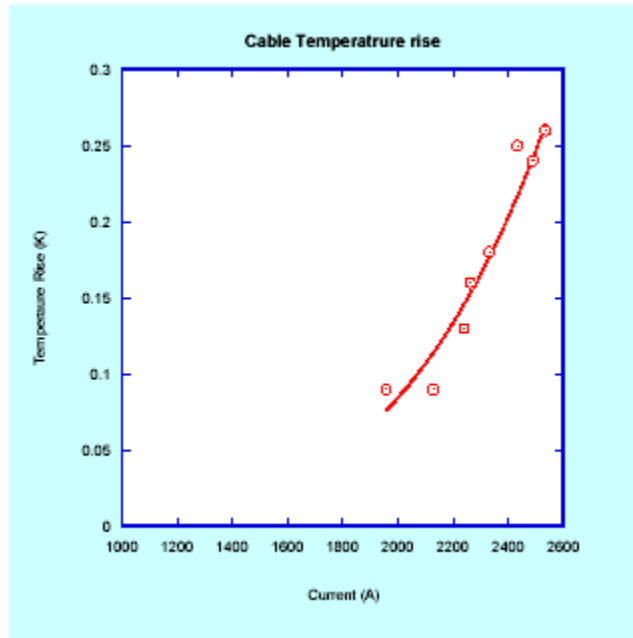


Figure 29. Cable temperature rise during ac loss test attempts

## **About EPRI**

EPRI creates science and technology solutions for the global energy and energy services industry. U.S. electric utilities established the Electric Power Research Institute in 1973 as a nonprofit research consortium for the benefit of utility members, their customers, and society. Now known simply as EPRI, the company provides a wide range of innovative products and services to more than 1000 energy-related organizations in 40 countries. EPRI's multidisciplinary team of scientists and engineers draws on a worldwide network of technical and business expertise to help solve today's toughest energy and environmental problems.

EPRI. Electrify the World

© 2004 Electric Power Research Institute (EPRI), Inc. All rights reserved. Electric Power Research Institute and EPRI are registered service marks of the Electric Power Research Institute, Inc. EPRI. ELECTRIFY THE WORLD is a service mark of the Electric Power Research Institute, Inc.

1002040



*Printed on recycled paper in the United States  
of America*